Steric Hindrance as a Basis for Structure-Based Design of Selective Inhibitors of Protein-Tyrosine Phosphatases†

Lars Fogh Iversen,*,‡,§ Henrik Sune Andersen,§,|| Karin Bach Møller,§,⊥ Ole Hvilsted Olsen,+ Günther H. Peters,@ Sven Branner,‡ Steen B. Mortensen,‡ Thomas Kruse Hansen,+ Jesper Lau,|| Yu Ge,# Daniel D. Holsworth,# Michael J. Newman,# and Niels Peter Hundahl Møller*,⊥

Protein Chemistry and Signal Transduction, Novo Nordisk, DK-2880 Bagsvaerd, Denmark, MedChem Research I and MedChem Research IV, Novo Nordisk, DK-2760 Måløv, Denmark, Chemistry Department, Technical University of Denmark, MEMPHYS, DK-2800 Lyngby, Denmark, and Ontogen Corporation, 2325 Camino Vida Roble, Carlsbad, California 92009

Received July 2, 2001; Revised Manuscript Received October 5, 2001

ABSTRACT: Utilizing structure-based design, we have previously demonstrated that it is possible to obtain selective inhibitors of protein-tyrosine phosphatase 1B (PTP1B). A basic nitrogen was introduced into a general PTP inhibitor to form a salt bridge to Asp48 in PTP1B and simultaneously cause repulsion in PTPs containing an asparagine in the equivalent position [Iversen, L. F., et al. (2000) *J. Biol. Chem. 275*, 10300−10307]. Further, we have recently demonstrated that Gly259 in PTP1B forms the bottom of a gateway that allows easy access to the active site for a broad range of substrates, while bulky residues in the same position in other PTPs cause steric hindrance and reduced substrate recognition capacity [Peters, G. H., et al. (2000) *J. Biol. Chem. 275*, 18201−18209]. The current study was undertaken to investigate the feasibility of structure-based design, utilizing these differences in accessibility to the active site among various PTPs. We show that a general, low-molecular weight PTP inhibitor can be developed into a highly selective inhibitor for PTP1B and TC-PTP by introducing a substituent, which is designed to address the region around residues 258 and 259. Detailed enzyme kinetic analysis with a set of wild-type and mutant PTPs, X-ray protein crystallography, and molecular modeling studies confirmed that selectivity for PTP1B and TC-PTP was achieved due to steric hindrance imposed by bulky position 259 residues in other PTPs.

Protein-tyrosine phosphatases (PTPs)[1] are a diverse family of enzymes that are critically involved in the regulation of signal transduction processes (reviewed in refs *1* and *2*). Both positive and negative effects on signal transduction have been attributed to specific PTPs. As an example, CD45 has been found to be essential for activation of T lymphocytes (*3*), whereas several enzymes have been proposed to be negative regulators of insulin signaling, including PTPα (*4*, *5*), PTP-LAR (*6*), and PTP1B (*7*, *8*). In particular, the intracellular PTP1B has recently received much attention in the latter respect. Independent results from two research groups have demonstrated that PTP1B knockout mice exhibit not only increased insulin sensitivity but also resistance to diet-induced obesity (*9*, *10*).

Considerable effort has recently been directed toward identification and design of selective PTP inhibitors. This is due to the demonstrated pivotal roles of PTPs as regulators of key signaling pathways and consequently their potential as drug targets (*11*). In addition, significant progress in our understanding of the molecular basis for substrate and inhibitor recognition by PTPs (*12*) allows structure-based drug design approaches to be utilized in this field (*13*).

Alignment of 113 full-length mammalian PTPs in combination with a so-called Cα variation score analysis indicates that the combination of residues 47, 48, 258, and 259 (PTP1B numbering, which is used throughout) constitutes a region that can be addressed for synthesis of selective PTP inhibitors (*14*). Using structure-based design, guided by PTP mutants and X-ray protein crystallography, we have recently shown that it is possible to obtain a high degree of inhibitor selectivity for PTP1B (*15*). This was achieved by introducing a basic nitrogen in the inhibitor core structure, resulting in formation of a salt bridge to the carboxy group of Asp48 in PTP1B and a concomitant repulsion in PTPs with an asparagine in the equivalent position.

However, since several other PTPs also contain an aspartic acid in position 48 (see Table 1), and consequently might be difficult against which to obtain selectivity, further optimization strategies are warranted. In this context, it is of interest that the bulky side chain of Gln259 in PTPα causes steric hindrance and reduced substrate recognition capacity (*16*). In PTP1B, this position is occupied by a glycine that, due to the lack of side chain atoms, allows easy

† G.H.P. was supported by Grant 97 100 05 from the Danish Cancer Society.

* To whom correspondence should be addressed. N.P.H.M.: e-mail, nphm@novonordisk.com. L.F.I.: e-mail, lfiv@novonordisk.com.

‡ Protein Chemistry, Novo Nordisk.

§ These authors contributed equally to this work.

|| MedChem Research I, Novo Nordisk.

⊥ Signal Transduction, Novo Nordisk.

+ MedChem Research IV, Novo Nordisk.

@ Technical University of Denmark.

Ontogen Corp.

[1] Abbreviations: PTP, protein-tyrosine phosphatase; pTyr and PY, phosphotyrosine; rms, root-mean-square.

10.1021/bi011389l CCC: $20.00
Published on Web 11/15/2001

Table 1: Amino Acid Residues in Positions 48, 258, and 259 (PTP1B Numbering)

residue	PTP1B	TC-PTP	SHP-1	PTPH1	PTPα	PTPϵ	CD45	PTP-LAR	PTPβ	GLEPP-1
48	Asp	Asp	Asn	Asp	Asn	Asn	Asp	Asn	Asn	Asn
258	Met	Met	Ser	Ala	Cys	Pro	Cys	Asn	Val	Met
259	Gly	Gly	Gly	Met	Gln	Gln	Leu	Tyr	His	Ser

access to the active site for a broad variety of substrates. We have termed this part of PTP1B the "258/259 gateway" to the active site or "region 258-259". It is positioned between Arg24 and Gln262, with Gly259 and Met258 forming the bottom of this cleftlike part of the enzyme. Since many PTPs have bulky side chains in position 259 and consequently restricted substrate recognition (see Table 1), we initiated this study to determine if the structural differences imposed by residue 259 could be employed in a novel structure-based approach to make selective inhibitors for PTP1B.

EXPERIMENTAL PROCEDURES

Cloning, Expression, and Purification. The following PTP domains were cloned, expressed, and purified as described previously (*15*, *17*): PTP1B, SHP-1, PTPα domain 1 (PTPαD1), PTPϵD1, CD45D1D2, PTP-LARD1D2, and PTPβ. cDNAs encoding TC-PTP (residues 1−314) (*18*), PTPH1 (residues 634−914) (*19*), and GLEPP1 (residues 885−1188) (*20*) were obtained by polymerase chain reaction using primers with convenient cloning sites and appropriate cDNA templates. The following PTP mutants were generated by overlap extension polymerase chain reaction using appropriate restriction sites for cloning purposes (*21*): PTP1B to PTPH1, (i) G259M; and PTPH1 to PTP1B, (ii) M259G. The following PTP1B and PTPα mutants were generated as described previously (*15*−*17*): PTP1B to PTPα, (iii) G259Q; and PTPα to PTP1B, (iv) Q259G. All constructs were inserted into pGEX expression vectors, expressed, and purified as described previously (*17*). All coding sequences were confirmed by DNA sequencing. For X-ray protein crystallography, the cDNA encoding the first 321 amino acids of PTP1B was inserted into the pET11a expression vector. PTP1B was purified in a two-step procedure: affinity purification using solid-phase-coupled compound **6** (see Figure 1) followed by anion exchange chromatography (unpublished experiments).

Determination of Inhibitor Constants. The enzyme reactions were carried out in microtiter plates at 25 °C essentially as described previously (*17*). In brief, appropriately diluted inhibitors (three or four different concentrations such as undiluted and diluted 3-, 9-, and 27-fold) were added to the reaction mixtures containing seven different concentrations of the substrate, *p*-nitrophenyl phosphate (range of 0.31−20 mM, final assay concentration). The assay buffer was 50 mM 3,3-dimethylglutarate, 1 mM EDTA, 1 mM dithiotreitol, and 0.1% (w/v) human serum albumin with the ionic strength adjusted to 0.15 M with addition of NaCl (final assay concentrations, total volume of 100 μL) (*22*). The reactions were started by addition of enzyme and quenched by addition of sodium hydroxide, and the enzyme activity was determined by measurement of A_{405} with appropriate corrections for the absorbance of the substrate and inhibitors. The data were analyzed using a nonlinear regression hyperbolic fit to classical Michaelis−Menten enzyme kinetic modes. The inhibitor constants, K_i (expressed in micromolar), are determined by replotting the apparent K_m values as a function of the inhibitor concentration (*23*). Experiments were repeated if the correlation coefficient R^2 was less than 0.98. Similar results were obtained independently with a three-component buffer system (*24*, *25*) consisting of Tris, Bis-Tris, and acetate (ionic strength of 100 mM) at pH 7.0 containing 0.1% (w/v) human serum albumin and 5 mM dithiothreitol (not shown).

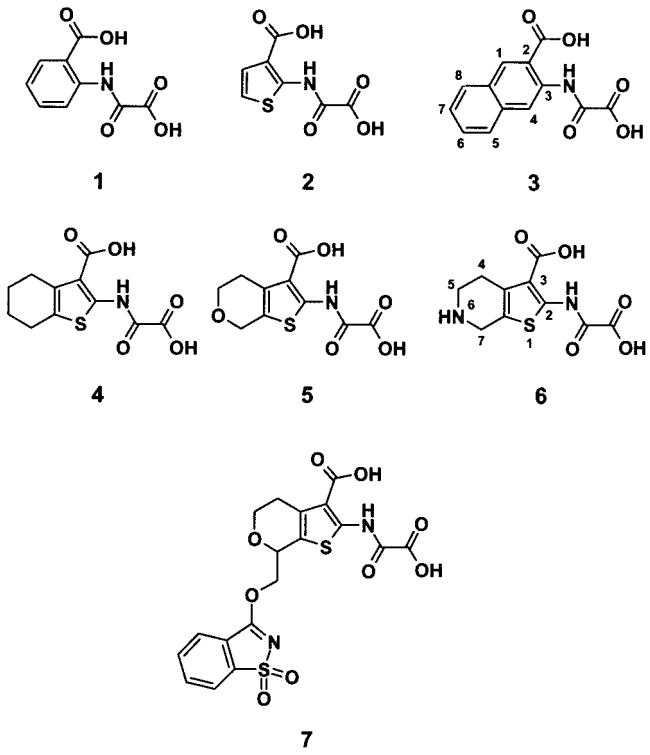

FIGURE 1: Chemical structures.

Crystallization. An approximately 10 mg/mL PTP1B protein solution in 10 mM Tris (pH 7.5), 25 mM NaCl, 0.2 mM EDTA, and 3 mM DTT was used for crystallization. Crystals were grown by the hanging drop vapor diffusion method. A 1:10 [PTP1B/compound **7** (see Figure 1)] molar ratio mixture was prepared at least 1 h prior to crystallization. Two microliters of the PTP1B/compound **7** solution was mixed with 2 μL of reservoir solution consisting of 0.1 M HEPES buffer (pH 7.5), 0.2−0.4 M sodium acetate or magnesium acetate, and 12−16% PEG 8000. The reservoir volume was 1 mL. Crystals grew to a size of 0.3 mm × 0.3 mm × 0.1−0.3 mm over 1 week.

Data Collection. One crystal was used for data collection, and diffraction data were collected at 100 K. The following cryo conditions were used. To the hanging drop was added 3 μL of 50% glycerol (containing 0.5 mmol of compound **7**). The crystal was removed from the drop after approximately 20 min and transferred to 50% glycerol (containing 0.5 mmol of compound **7**) and flash-frozen. Data were collected using a Mar345 image plate detector on a rotating

Table 2: Statistics of X-ray Data and Structure Refinements

space group	*P*3121
unit cell parameters	$a = b = 88.3$ Å, $c = 103.6$ Å
completeness (20−2.50 Å)	98.9%
completeness (2.54−2.50 Å)	97.5%
multiplicity (20−2.50 Å)	4.1
R_{merge} (20−2.50 Å)	9.1%
R_{merge} (2.54−2.50 Å)	30.2%
$\langle I/\sigma(I)\rangle$ (20−2.50 Å)	10.1
$\langle I/\sigma(I)\rangle$ (2.54−2.50 Å)	3.1
no. of unique reflections	16416
no. of atoms in structure	2594
R-factor[a]	18.9
R_{free}[b]	27.0
rms deviations from idealized geometry	
bond lengths (Å)	0.018
bond angles (deg)	3.7
dihedral angles (deg)	2.2

[a] *R*-factors were calculated using all data from 6 to 2.50 Å. Crystallographic *R*-factor $= \sum_{(hkl)}||F_o| - |F_c||/\sum_{(hkl)}|F_o|$. [b] $R_{free} = \sum_{(hkl)\epsilon T}||F_o| - |F_c||/\sum_{(hkl)\epsilon T}|F_o|$, where T is a test set containing a random 5% of the observations omitted from the refinement process.

anode (RU300, Cu Kα, 50 kV and 80 mA) equipped with an Osmic multilayer mirror system. A 1° oscillation per image was used for 70 images. A data set to 2.5 Å resolution was obtained. The space group was determined to be *P*3121. Data processing was performed using Denzo, Scalepack, and the CCP4 program suite (*26*, *27*).

Refinements. As the *P*3121 space group contains a polar axis and thus possesses more than one indexing possibility, a molecular replacement solution using Amore (*27*, *28*) was determined prior to the refinements. A high-resolution PTP1B structure was used as a starting model (*17*), with ligand and water molecules omitted from the structure. All refinements were performed with Xplor version 3.851 [Molecular Simulations Inc. (MSI)]. Interchanging cycles of model building using X-build (MSI) and refinement were performed. The $2F_o - F_c$ maps were inspected by the use of X-ligand (MSI) at a 1.0σ level for densities that could correspond to the structures of compound **7**. An electron density map well suited for compound **7** was identified in the active site pocket. No other densities were identified to fit compound **7**. Water molecules were inserted using the X-solvate program (MSI). The graphical interface that was used was Quanta (MSI). For further details, see Table 2.

Compound Synthesis. The preparation of compound **5** has been described previously (*15*). 2-Amino-7-(hydroxymethyl)-4,7-dihydro-5*H*-thieno[2,3-*c*]pyran-3-carboxylic acid *tert*-butyl ester was coupled under Mitsunobu conditions with 1,1-dioxo-1,2-dihydro-1*H*-benzo[*d*]isothiazol-3-one (saccharine), affording 2-amino-7-(1,1-dioxo-1*H*-benzo[*d*]isothiazol-3-yloxymethyl)-4,7-dihydro-5*H*-thieno[2,3-*c*]pyran-3-carboxylic acid *tert*-butyl ester as an oil, which was reacted with midazol-1-yl oxoacetic acid *tert*-butyl ester, affording 2-(*tert*-butoxyoxalylamino)-7-(1,1-dioxo-1*H*-benzo[*d*]isothiazol-3-yloxymethyl)-4,7-dihydro-5*H*-thieno[2,3-*c*]pyran-3-carboxylic acid *tert*-butyl ester as an oil. Treatment of the bis-*tert*-butyl ester with 50% TFA in dichloromethane afforded 7-(1,1-dioxo-1*H*-benzo[*d*]isothiazol-3-yloxymethyl)-2-(oxalylamino)-4,7-dihydro-5*H*-thieno[2,3-*c*]pyran-3-carboxylic acid (compound **7**) as a solid: mp 234−236 °C.

Molecular Modeling. The molecular mechanics package MacroModel (*29*) was used to evaluate the conformational energy of the bound ligand structure relative to the global energy minimum or other local minima. The MMFF force field as implemented in MacroModel was employed with default settings. All calculations were carried out on an SGI challenge computer. First, the conformational space was searched using the Monte Carlo multiple method (*30*). The energy minimizations were carried out using the truncated conjugate algorithm using a model for aqueous solution [i.e., a generalized Born, solvent accessible surface area continuum dielectric solvation model (*31*)]. The conformational searches were continued until all low-energy minima had been found multiple times. Second, the energy of the ligand in the conformation observed in the X-ray structure was estimated. The crystallographic structure was partially relaxed in the force field. A set of heavy atoms was tethered to the crystallographic positions by harmonic flat-bottomed Cartesian constraints. The flat-bottomed radius was 0.3 Å, i.e., the distance each atom is allowed to move from the tether position before an energy penalty is applied. At larger distances, a harmonic penalty function with a force constant of 500 kJ mol^{-1} $Å^{-2}$ was applied. The two carboxylic acid groups of compound **7** were omitted in the calculations since no structural variations have ever been observed in these parts of the inhibitors (*15*−*17*).

A database search in IsoStar (*32*) was conducted to examine the frequency of observed short distances between sulfone oxygens and carbonyls, carbon, and sulfate atoms. IsoStar is a library of information about intermolecular interactions based on experimental information from the Cambridge Structural Database and the Protein Data Bank.

RESULTS

Whereas a glycine in position 259 in PTP1B and TC-PTP leads to easy accessibility to the active site and concurrent broad substrate binding capacity, many other PTPs with bulky side chains in the equivalent position are rather limited in their capacity to recognize substrates (see Table 1) (*16*). Therefore, we reasoned that these observations could be used in structure-based design of inhibitors that are selective for PTP1B and TC-PTP. We have recently shown that compounds containing two carboxy groups bound, directly or via a carbonylamino group, to an aromatic ring will function as general PTP inhibitors (Figure 1, compounds **1** and **2**) (*17*). In agreement with observations made on phosphonate-based PTP inhibitors by others (*33*), we found that an additional aromatic or saturated ring significantly increased the general potency (Figure 1, compounds **3** and **4**) (*15*, *17*). On the basis of X-ray protein crystallographic studies of PTP1B complexed with these inhibitors, such fused ring systems containing the above carboxy groups seemed to be suitable starting points for structure-based design of inhibitors addressing region 258-259 of PTP1B.

Selection of the Synthetic Scaffold and Inhibitor Design. We hypothesized that an appropriate substituent in position 5 of compound **3** or in position 7 in compounds **4**−**6** would be able to bind in region 258-259 of PTP1B and other PTPs with an open 258/259 gateway, whereas such inhibitors would be prevented from binding to PTPs with bulky side chains in position 259 due to steric hindrance. Consequently, such inhibitors should have improved affinity for PTP1B and TC-PTP and almost the same or lower affinity as the parent compounds (without substituents) against PTPs with a blocked 258/259 gateway.

Table 3: K_i Values (μM) at pH 7.0

	wt PTP1B	PTP1B G259Q	PTP1B G259M	wt PTPα	PTPα Q259G	wt PTPH1	PTPH1 M259G
compound **5**	84	486	329	>500	128	246	121
compound **7**	0.6	108	53	>500	58	91	19

Incorporation of a basic nitrogen into 2-(oxalylamino)-4,5,6,7-tetrahydrobenzo[*b*]thiophene-3-carboxylic acid (Figure 1, compound **4**) results in a highly selective inhibitor of PTP1B, compound **6**, due to formation of a salt bridge with Asp48 (*15*). In accordance with the above predictions, introduction of an appropriate substituent into position 7 of compound **6** should result in inhibitors that address the 258/259 gateway. However, since compound **6** is already highly selective for PTP1B, a scaffold without the basic nitrogen (i.e., compound **3**, **4**, or **5**) would be required to allow unequivocal evaluation of the influence of substituents that could address the 258/259 gateway with respect to selectivity. The lessons learned from these scaffolds can probably be used to further optimize other synthetic starting points, such as compound **6**, and hence lead to compounds with even higher potency and selectivity.

Comparison of compounds **3**−**5** against a set of wild-type (wt) PTPs revealed almost identical inhibitory profiles, and therefore, all three constitute potentially suitable synthetic scaffolds (*15*; not shown). However, closer inspection of the crystal structure of PTP1B complexed with compound **3** revealed that introduction of a substituent at position 5 of this compound most likely would lead to steric collision with Ile219 and Val49 (not shown). In contrast, provided that the saturated ring of compound **5** is in a twisted boat conformation with the oxygen atom pointing upward, position 7 substitutions should lead to compounds addressing the 258/259 gateway of PTP1B. Due to the above and to the ease of synthesis, compound **5** was subsequently selected as a scaffold for further synthesis.

Our aim was to make inhibitors that would "pass through" the 258/259 gateway and simultaneously bind to the side chains or main chain structures in the vicinity of residue 259. In particular, we wanted to address the conserved Gln262 side chain and the hydrophobic pocket around Met258 in PTP1B. Several compounds were synthesized. The structure of one of these, compound **7**, is shown in Figure 1. In comparison with the parent compound (**5**), this inhibitor exhibited an approximately 100-fold increase in affinity for PTP1B (Table 3). Importantly, compound **7** acts as a classical competitive inhibitor as exemplified in Figure 2.

PTP Mutants. To test if compound **7** addresses the proposed region of PTP1B, we performed detailed enzyme kinetic analyses using a set of wt and mutant PTPs. Two enzymes, PTPα and PTPH1, were chosen as representatives for PTPs with bulky side chains in position 259. Using a similar approach with a combination of wt and PTP mutants, we have previously demonstrated that Gln259 in PTPα, in addition to its direct effect, also indirectly influences the binding of inhibitors and substrates, most likely due to a negative influence on the rotational freedom of the side chain of Gln262 (*16*). As described above, selectivity can be obtained by introducing a basic nitrogen into compound **4** (Figure 1) that causes attraction in PTP1B due to formation of a salt bridge to Asp48 and repulsion against PTPs with

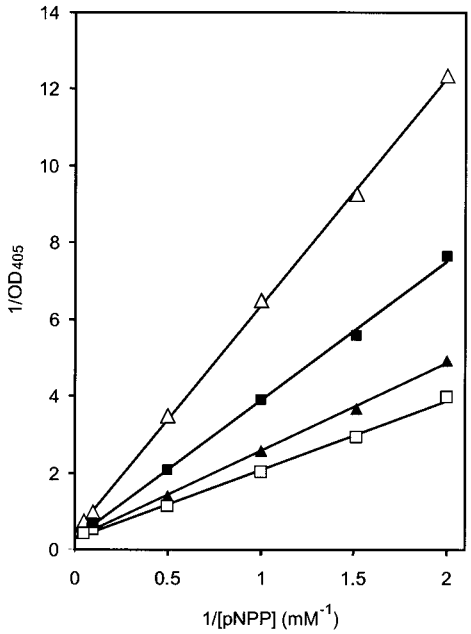

FIGURE 2: Compound **7** is a classical, competitive inhibitor of PTP1B. Michaelis−Menten curves: (□) no addition of compound **7** and (▲) 0.33, (■) 1, and (△) 3.0 μM compound **7**.

an asparagine in the 48 position, such as PTPα. Although this is an attractive approach for selectivity against "Asn48-PTPs", it should be noted that several PTPs contain an aspartic acid in position 48. Therefore, to analyze if the current approach based on steric hindrance is generally applicable, we decided to include a PTP with an Asp in position 48 ("Asp48-PTPs"). PTPH1, which like PTP1B is an intracellular enzyme with one catalytic domain only, was selected as a representative for these enzymes. Of note, residue 259 in PTPH1 is a methionine similar in size to the glutamine in PTPα. Therefore, although the crystal structure of PTPH1 is not available, we hypothesized that the 258/259 gateway in PTPH1 would be blocked as in PTPα. On the other hand, the adjacent residue 258 is an alanine that might allow more rotational freedom of Met259 in PTPH1 than of Gln259 in PTPα with its neighboring Cys258.

The inhibitory profile of compound **7** was compared with that of the parent compound **5** (Table 3). In agreement with our previous findings with low-molecular weight inhibitors (*16*), introduction of bulky side chains in position 259 in PTP1B (corresponding to PTPα and PTPH1, respectively) causes only a modest 4−6-fold decrease in affinity for compound **5**. In contrast, a very significant decrease in affinity was observed for compound **7** when comparing wt and mutant forms of PTP1B (Table 3). Therefore, these results clearly show that a glutamine or a methionine in position 259 is sufficient to prevent high-affinity binding of compound **7** and further support the hypothesis that compound **7** addresses region 258-259 in PTP1B. In contrast, compounds **5** and **7** showed almost the same affinity for the PTPα Q259G mutant, indicating that removal of the steric hindrance imposed by Gln259 is not enough to restore full binding capacity, i.e., comparable to that of PTP1B, for compound **7**. This is not a surprising observation since this would require the same possibilities for ligand binding in the PTPα mutant enzyme and wt PTP1B. One important difference between these enzymes is residue 48, which is an asparagine in PTPα. In contrast to the equivalent aspartic

Table 4: K_i Values (μM) at pH 7.0

	PTP1B	TC-PTP	SHP-1	PTPH1	PTPα	PTPε	CD45	PTP-LAR	PTPβ	GLEPP-1
compound **5**	84	111	>500	246	>500	>500	>1000	>1000	100	238
compound **7**	0.6	1.1	289	91	>500	>500	489	176	21	370

acid in PTP1B, the side chain of this residue cannot form water-mediated hydrogen bonds similar to those found between compound **7** and PTP1B (see below). Further, the shorter side chain of Cys258 in PTPα, in comparison with the methionine in the equivalent position in PTP1B, is probably not capable of making van der Waals contacts to the ligand. Therefore, the observed selectivity of compound **7** for PTP1B versus PTPα seems to be due to (i) steric hindrance in the latter and (ii) better possibilities for contact between the ligand and PTP1B. Although compound **7** binds with somewhat higher affinity than compound **5** to wt PTPH1 and the PTPH1 M259G mutant, similar conditions are likely to be at play in PTPH1 that contains an alanine in position 258. Since PTPH1 contains an aspartic acid in position 48 and hence the potential for the above hydrogen bond formation, we reason that the saccharin ligand moiety of compound **7** is guided into the 258/259 gateway. It should be emphasized that the observed increase in affinity of compound **7** versus compound **5** for both the wt and mutant PTPH1 enzymes is modest (2−6-fold) compared to that observed for PTP1B (140-fold). Thus, the fine architecture seems to be different in these enzymes, even when the bulky Met259 residue in PTPH1 has been substituted for a glycine.

Specificity against a Broad Set of PTPs. Having provided evidence that compound **7** indeed was addressing the 258/259 gateway of PTP1B, we next determined if the side chain of the compound would cause the hypothesized increased selectivity against other PTPs. Compounds **5** and **7** were tested against a set of 10 different wt PTP domains (Table 4). With the exception of PTP1B and TC-PTP, compound **7** showed modest or no inhibition of these enzymes and only a 5-fold increase in affinity for PTPβ in comparison with that of compound **5**. Thus, we have succeeded in obtaining a substantial increase in affinity for PTP1B and TC-PTP, and simultaneously introduce a very high degree of selectivity against many other PTPs representing a broad spectrum of this class of enzymes. Significantly, this selectivity is also found against two PTPs that contain an aspartic acid in position 48, i.e., CD45 and PTPH1.

The observed selectivity against SHP-1 is in apparent contradiction to our hypothesis regarding steric hindrance, since this enzyme has a glycine in position 259. However, as will be discussed below, water-mediated hydrogen bonds from compound **7** to the side chain of Asp48 in PTP1B play a significant role in obtaining potency against PTP1B. It is unlikely that similar interactions can take place in Asn48-PTPs such as SHP-1.

X-ray Protein Crystallography. As shown above, the enzyme kinetic analyses with wt and mutant PTPs indicated that compound **7** interacts with region 258-259. To determine unequivocally the binding mode, we next initiated cocrystallization studies of PTP1B and compound **7**. A well-suited electron density was identified in the active site pocket (Figure 3). The oxalylamino and *o*-carboxy groups show the exact same interaction with the PTP signature motif and formation of a salt bridge to Lys120 as described previously

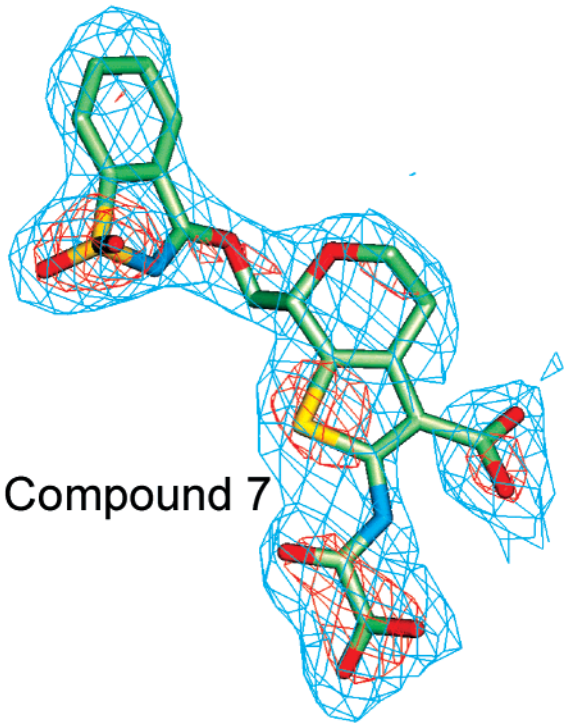

FIGURE 3: Binding mode of compound **7** in PTP1B. Omit maps ($2F_o - F_c$) for the PTP1B−compound **7** complex structure. The electron density maps are contoured in blue at the 1σ level and in red at the 3σ level. The inhibitor has been omitted from the phasing model and refined for several cycles before map calculation. Atoms are colored according to atom type (carbons in green, oxygens in red, sulfurs in yellow, and nitrogens in blue).

for 2-(oxalyamino)benzoic acid and the thiophene-based derivatives (*15*−*17*). Superimposition of the complex structures of compound **5** and compound **7** shows complete overlap of the aromatic and pyran rings (Figure 4). Significantly, and as predicted, the side chain of the ligand is positioned in the vicinity of residues 258 and 259 (Figures 4 and 5A). Several interaction points seem to explain the observed significant increase in the affinity of compound **7** for PTP1B. Although we were not successful in obtaining interaction with Gln262 and no hydrogen bonds are seen from the saccharin ligand moiety to the protein, important van der Waals contacts are observed between the saccharin and several residues of the protein, including Asp48, Val49, Ile219, Met248, and Gly259.

Unexpectedly, we also observe three short distances, not of hydrogen bond nature, from the sulfone oxygens in the saccharin to the backbone carbonyl of Asp48 (3.2 Å), a sulfur atom in Met258 (3.1 Å), and a Cα atom in Gly259 (3.2 Å) that are not readily accounted for (see also Figure 5A). To determine if such interactions have been observed previously, we performed a search in the IsoStar database. Interactions comparable to those observed between compound **7** and the backbone carbonyl of Asp48 and the Cα atom of Gly259 were frequently observed in IsoStar (data not shown), whereas the interaction with the sulfur atom in Met258 apparently has not been described before. It should be

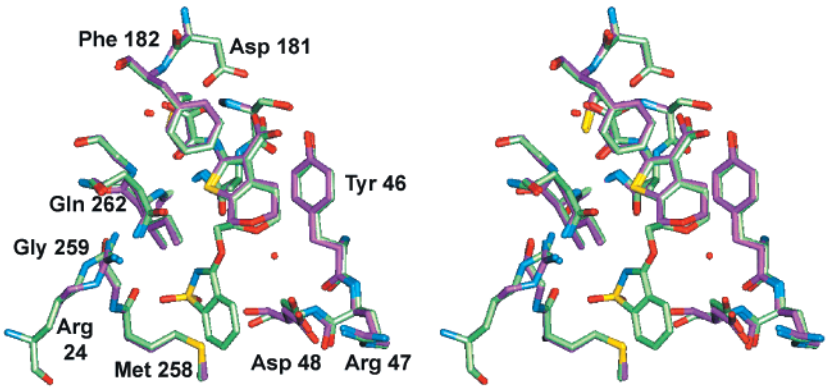

FIGURE 4: Superimposition of the PTP1B−compound **5** and PTP1B−compound **7** structures (stereoview). The structures were superimposed using Quanta (MSI). Atoms are colored according to atom type (carbons in green for the complex with compound **5** and magenta for the complex with compound **7**, oxygens in red, sulfurs in yellow, and nitrogens in blue).

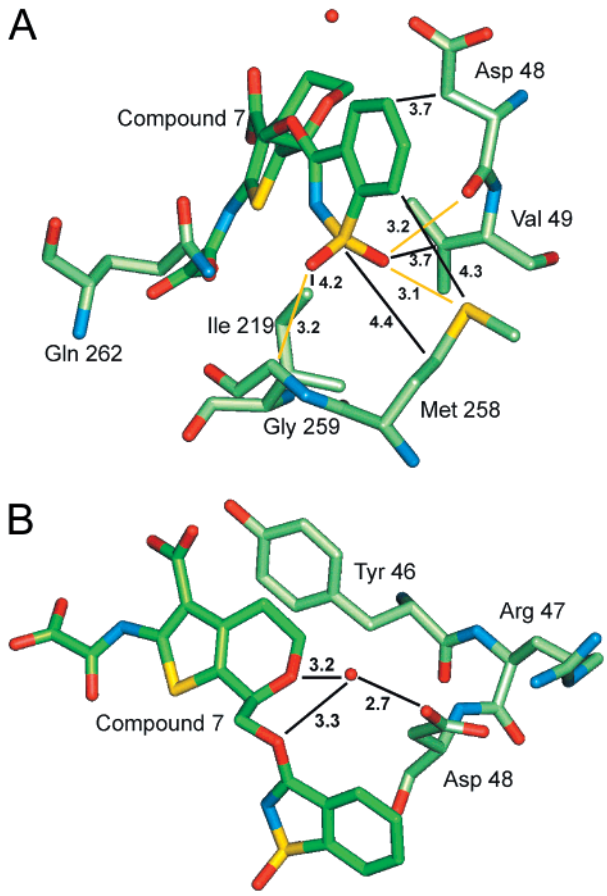

FIGURE 5: Binding mode of compound **7**. (A) van der Waals contact between the saccharin moiety and PTP1B. Short non-hydrogen interactions are colored in yellow. (B) Water-mediated interaction with Asp48.

emphasized that the sulfone in saccharin is the most electron rich part of the inhibitor and hence the best defined part of the ligand in the electron density maps (see Figure 3). Consequently, the saccharin moiety is accurately determined in the complex structure.

With the current data in hand, it is difficult to evaluate the influence of these three short interactions on binding affinity. However, since the total area is quite electron rich with several unpaired lone pairs, i.e., the sulfone on one side and the carbonyl and methionine sulfur atoms on the other, a negative net effect on binding affinity is expected.

Aspartic Acid 48. As discussed above, we have previously utilized formation of a salt bridge to Asp48 to obtain potent and selective PTP1B inhibitors (*15*). In this case, Asp48 was in the so-called rotamer 3 position, pointing toward the active site. In contrast, the side chain of Asp48 is pushed away from the active site by the oxygen atom in the pyran ring in the complex structures with compounds **5** and **7** (i.e., to the rotamer 1 position). This allows a water molecule not seen in previous complex structures to form a hydrogen-bonded bridge between the two oxygen atoms in the ligand and Asp48 (Figure 5B). It is conceivable that this water molecule-mediated interaction with Asp48 in combination with the above-mentioned van der Waals contact accounts for the significant increase in the affinity of compound **7** for PTP1B in comparison with that of compound **5**.

The above-described water-mediated hydrogen bonds to the side chain of Asp48 in PTP1B complexed with compound **7** also provide a likely explanation for the apparent contradictory finding of selectivity against SHP-1, which has a glycine in position 259. As pointed out by us previously (*15*), the Asn48 residues in the published Asn-PTPs are in the rotamer 3 position with an internal hydrogen bond to the neighboring backbone amide (*34*−*36*). Further, using a PTP1B mutant, we have shown that the oxygen atom in the pyran ring of compound **5** attracts Asn48 and stabilizes the side chain of this residue in the rotamer 3 position. Therefore, such water-mediated hydrogen bond formation in SHP-1 is unlikely. In agreement with this, we find compound **7** to inhibit SHP-1 with a relatively low affinity. It should be noted, however, that compound **7** is more potent than compound **5** against SHP-1, thus indicating that some binding affinity has been obtained in the 258/259 gateway of this enzyme.

Binding to PTPs with Bulky Side Chains in Position 259 (Low-Energy Conformations). The conformation of compound **7** found in the X-ray structure with PTP1B is a low-energy conformation with an estimated energy of 102.9 kJ/mol (data not shown). Significantly, the low-energy conformation obtained after flat-bottomed minimization is almost identical to the observed X-ray conformation (see Figure 6A). When binding to PTPs with bulky residues in position 259, compound **7** has to either differ from this minimum low-energy conformation or force the bulky side chain away (i.e., to keep the low-energy conformation). In both cases, an energy penalty will arise.

Since no complex structure is available for PTPs with a blocked 258/259 gateway, e.g., PTPα, we have previously used a PTP1B mutant (R47V, D48N, M258C, and G259Q) as a model for such enzymes (*15*). The X-ray structure of this PTP1B mutant was used here to identify alternative low-energy conformations of compound **7** that could be accommodated in PTPs with bulky residues in position 259 (Figure 6B). The estimated conformational energy in this case is 106.8 kJ/mol, representing a significant energy penalty of 3.9 kJ/mol. Thus, such an increase in conformational energy would lead to a significant estimated loss in affinity, i.e., corresponding to the experimentally observed decrease in the affinity of compound **7** for PTP1B G259Q (Table 3). Of note, this PTP1B mutant still binds compound **7** with a considerably higher affinity than PTPα, perhaps reflecting a water-mediated interaction with Asp48 similar to that described above for wt PTP1B.

The global energy minimum for compound **7** was estimated to be 100.8 kJ/mol using the MMFF force field. However, it should be stressed that it is not possible to dock this conformation into PTP1B or the above PTP1B mutant serving as a model for enzymes with a blocked 258/259 gateway (*15*).

DISCUSSION

Ligand selectivity can be obtained by using several interaction types between the protein target and ligand molecules. To keep the molecular weight low, we generally attempt to increase the selectivity by simultaneously increasing the potency for the desired target, e.g., PTP1B, while decreasing the affinity against nontarget enzymes. Previously, we reported the design of a selective PTP1B inhibitor using electrostatic attraction in PTP1B and repulsion in undesired target PTPs (*15*). Here we demonstrate that the combined use of steric fit and steric hindrance is a powerful tool in structure-based ligand design. Using a multiple alignment of PTPs and structural analyses, the region around residues 258 and 259 (termed the 258/259 gateway) was identified as a region in PTPs with characteristics for possible selectivity design based on steric features (Figure 7). In PTP1B and TC-PTP, residue 259 is a glycine that results in an open 258/259 gateway. In a substantial number of other PTPs, position 259 is occupied by a residue with a bulky side chain. As an example, PTPα has a Gln in position 259, and thus a closed 258/259 gateway. By extending our inhibitors toward the 258/259 gateway, we speculated that PTP1B and TC-PTP could easily accommodate the substituents with increased binding affinity as a result, whereas other PTPs with closed 258/259 gateways would be less prone to binding such inhibitors. Compound **7** was synthesized, and the binding mode was evaluated by detailed enzyme kinetic analysis with a set of mutant PTPs as well as with X-ray protein crystallography. Further, this approach also resulted in a compound with remarkable selectivity against a series of PTPs representing both intracellular and receptor-like enzymes.

The increase in potency obtained by introducing a substituent in position 7 of compound **5** seems to be due to a combination of (i) van der Waals interactions for the saccharin part and (ii) formation of water-mediated hydrogen bonds from the oxygen atom in the pyran ring as well as the ether oxygen in compound **7** to the side chain of Asp48. In PTPs with an asparagine in the equivalent position, such interaction is unlikely to occur due to a preference for the rotamer 3 position of this residue (i.e., pointing toward the active site). Therefore, this water-mediated interaction with Asp48 may also contribute to the observed selectivity of compound **7** against PTPs in which residue 48 is an asparagine. In accordance with this, compound **7** is a weak inhibitor of SHP-1 despite the fact that this enzyme has a glycine in position 259, i.e., an open 258/259 gateway (*36*, *37*).

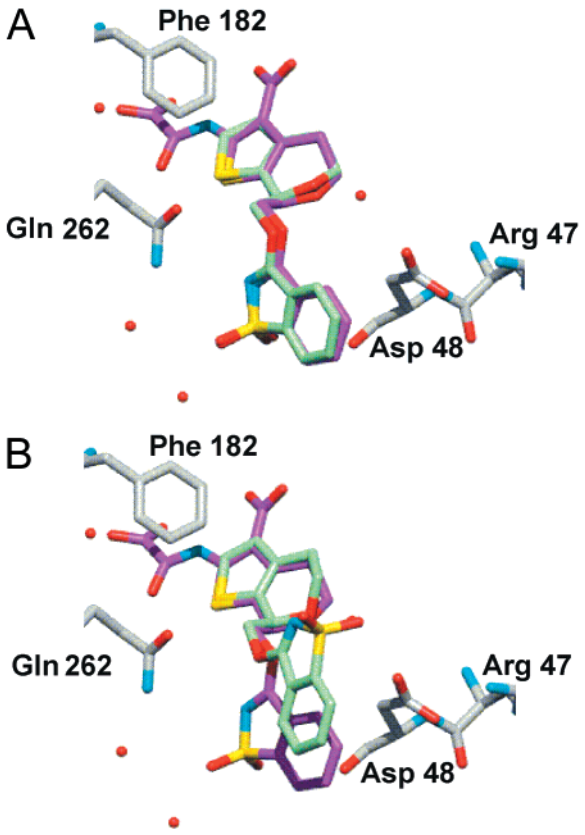

FIGURE 6: Low-energy conformation of compound **7**. (A) Superimposition of the calculated low-energy conformation of compound **7** and the observed conformation of compound **7** (in magenta) complexed with PTP1B. (B) Suggested binding mode of compound **7** in PTPs with bulky side chains in position 259. As in panel A, the model has been compared to the observed conformation of compound **7** complexed with PTP1B.

Ligands may change conformation upon binding. Thus, the conformation of the protein-bound ligand does not necessarily represent the global minimum for the free ligand. However, such a conformation may result in energy penalties that significantly affect the binding affinity. Indeed, each 5.6 kJ/mol of increased conformational energy of the bound conformation leads to a loss in affinity of a factor of 10 (*38*). When binding to PTPs with 259 residues with bulky side chains, the conformation for compound **7** has to either force the position 259 side chain away to keep the low-energy conformation or attain a different conformation. In both cases, an increased energy penalty will be the result, as also demonstrated in the enzyme kinetic analyses. Of note, Monte Carlo analysis of compound **7** revealed that the energy of the low-energy conformation in PTP1B is 3.9 kJ/mol lower than a conformation of the compound fitting in PTPs with bulky side chains.

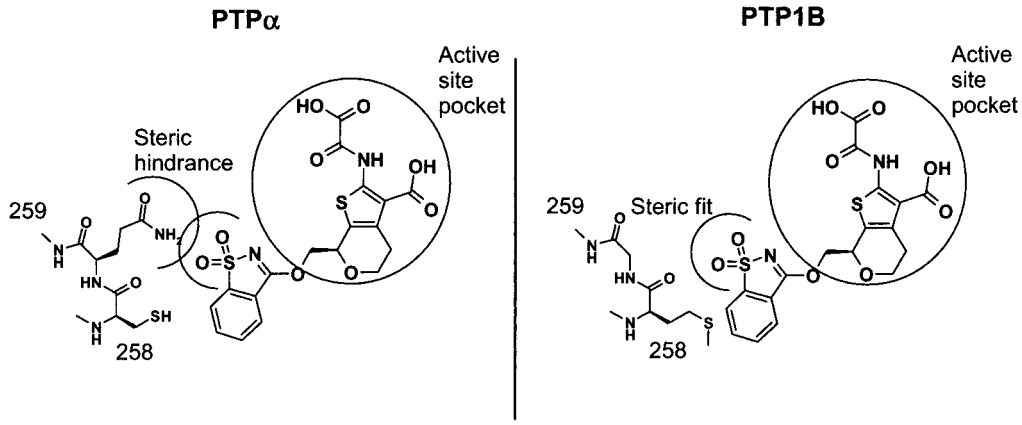

FIGURE 7: Schematic illustration of the closed and open 258/259 gateways in PTPα and PTP1B, respectively.

Zhang and co-workers have recently identified a second aryl phosphate binding site in PTP1B (*39*). The most important residues in this site seem to be Arg24 and Arg254 with the guanidinium groups of these residues coordinating the phosphate group of phosphotyrosine. While Arg254 is a highly conserved residue, Arg24 seems to be present in only a few PTPs, including TC-PTP and PTP-PEST. It is, therefore, tempting to speculate that selective and potent inhibitors can be obtained by concurrently addressing the active site and the second aryl phosphate binding site. Further, if such compounds also have to pass through the 259/259 gateway, we have provided evidence that such inhibitors should be highly selective. Although no structural information was provided, it is of specific interest in this context that the same research group has been able to synthesize highly selective and potent phosphonate-based PTP1B inhibitors by attempting to reach the active site and the second aryl binding site simultaneously (*40*).

PTP1B has recently been the focus of significant research activities due to its proposed role as a major negative regulator of insulin signaling. In particular, two studies on PTP1B knockout mice have convincingly demonstrated that selective PTP1B inhibitors potentially could be important therapeutics for the treatment of diabetes (*9*, *10*). Further, a blood glucose lowering effect, to almost normal levels, has been achieved in ob/ob and db/db mice by treatment with PTP1B antisense oligonucleotides once a week for a total of 4 weeks (Brett Monia, ISIS Pharmaceuticals; personal communication). In accordance with several in vitro studies (*7*, *41*), it was found in one of the above reports on PTP knockouts that the insulin receptor itself might be an important substrate for PTP1B. In this context, it is of significant interest that the X-ray structure of PTP1B in complex with a triply phosphorylated synthetic peptide corresponding to the insulin receptor tyrosine kinase activation loop exhibited simultaneous binding to the active site and the second aryl phosphate binding site (*42*). This dual binding mode is only possible with the substrate positioned in the 258/259 gateway, as demonstrated by the fact that the peptides with two adjacent pTyr molecules, i.e., the IR peptide, show much lower binding affinity to PTP1B mutants with bulky side chains in position 259. In other words, our design strategy for selective PTP1B inhibitors presented here seems to mimic Nature's way of obtaining substrate selectivity.

We hypothesize that by combining the present approach based on steric fit and steric hindrance (residue 259) with the previously described utilization of attraction and repulsion (residue 48) (*15*), highly potent and selective PTP1B inhibitors can be developed. However, it should be emphasized that such inhibitors most likely will also bind to TC-PTP, which is highly homologous to PTP1B. To obtain selectivity against TC-PTP, other areas of the enzymes have to be addressed.

ACKNOWLEDGMENT

The expert technical assistance of Lise Lotte Nilausen Schmidt, Annette L. Peulicke Sørensen, and Annette S. Petersen is greatly appreciated. We thank Dr. Kjeld Norris for providing wt GLEPP-1 and PTPα mutant expression vectors and the following colleagues for helpful discussions: Drs. Behrend F. Lundt, James G. McCormack, and Hanne B. Rasmussen at Novo Nordisk and Drs. Roy Uyeda and William C. Ripka at Ontogen Corp.

REFERENCES

1. Hunter, T. (2000) *Cell 100*, 113−127.
2. Hunter, T. (1998) *Philos. Trans. R. Soc. London, Ser. B 353*, 583−605.
3. Thomas, M. L., and Brown, E. J. (1999) *Immunol. Today 20*, 406−411.
4. Møller, N. P. H., Møller, K. B., Lammers, R., Kharitonenkov, A., Hoppe, E., Wiberg, F. C., Sures, I., and Ullrich, A. (1995) *J. Biol. Chem. 270*, 23126−23131.
5. Jacob, K. K., Sap, J., and Stanley, F. M. (1998) *J. Biol. Chem. 273*, 4800−4809.
6. Goldstein, B. J. (1992) *J. Cell. Biochem. 48*, 33−42.
7. Kenner, K. A., Anyanwu, E., Olefsky, J. M., and Kusari, J. (1996) *J. Biol. Chem. 271*, 19810−19816.
8. Ahmad, F., Li, P.-M., Meyerovitch, J., and Goldstein, B. J. (1995) *J. Biol. Chem. 270*, 20503−20508.
9. Elchebly, M., Payette, P., Michaliszyn, E., Cromlish, W., Collins, S., Loy, A. L., Normandin, D., Cheng, A., Himms-Hagen, J., Chan, C.-C., Ramachandaran, C., Gresser, M. J., Tremblay, M. L., and Kennedy, B. P. (1999) *Science 283*, 1544−1548.
10. Klaman, L. D., Boss, O., Peroni, O. D., Kim, J. K., Martino, J. L., Zabolotny, J. M., Moghal, N., Lubkin, M., Kim, Y. B., Sharpe, A. H., Stricker-Krongrad, A., Shulman, G. I., Neel, B. G., and Kahn, B. B. (2000) *Mol. Cell. Biol. 20*, 5479−5489.
11. Møller, N. P. H., Iversen, L. F., Andersen, H. S., and McCormack, J. G. (2000) *Curr. Opin. Drug Discovery Dev. 3*, 527−540.

12. Burke, T. R., Jr., and Zhang, Z.-Y. (1998) *Biopolymers 47*, 225−241.
13. Dalgarno, D. C., Metcalfe, D. D., Shakespeare, W. C., and Sawyer, T. K. (2000) *Curr. Opin. Drug Discovery Dev. 3*, 549−564.
14. Andersen, J. N., Mortensen, O., Peters, G. H., Drake, P. G., Iversen, L. F., Olsen, O. H., Andersen, H. S., Tonks, N. K., and Møller, N. P. H. (2001) *Mol. Cell. Biol. 21*, 7117−7136.
15. Iversen, L. F., Andersen, H. S., Branner, S., Mortensen, S. B., Peters, G. H., Norris, K., Olsen, O. H., Jeppesen, C. B., Lundt, B. F., Ripka, W., Møller, K. B., and Møller, N. P. H. (2000) *J. Biol. Chem. 275*, 10300−10307.
16. Peters, G. H., Iversen, L. F., Branner, S., Andersen, H. S., Mortensen, S. B., Olsen, O. H., Møller, K. B., and Møller, N. P. H. (2000) *J. Biol. Chem. 275*, 18201−18209.
17. Andersen, H. S., Iversen, L. F., Jeppesen, C. B., Branner, S., Norris, K., Møller, K. B., and Møller, N. P. H. (2000) *J. Biol. Chem. 275*, 7101−7108.
18. Cool, D. E., Tonks, N. K., Charbonneau, H., Walsh, K. A., Fischer, E. H., and Krebs, E. G. (1989) *Proc. Natl. Acad. Sci. U.S.A. 86*, 5257−5261.
19. Yang, Q., and Tonks, N. K. (1991) *Proc. Natl. Acad. Sci. U.S.A. 88*, 5949−5953.
20. Wiggins, R. C., Wiggins, J. E., Goyal, M., Wharram, B. L., and Thomas, P. E. (1995) *Genomics 27*, 174−181.
21. Horton, R. M., Hunt, H. D., Ho, S. N., Pullen, J. K., and Pease, L. R. (1989) *Gene 77*, 61−68.
22. Sarmiento, M., Zhao, Y., Gordon, S. J., and Zhang, Z.-Y. (1998) *J. Biol. Chem. 273*, 26368−26374.
23. Copland, R. A. (1996) Reversible Inhibitors, *Enzymes: A Practical Introduction to Structure, Mechanism and Data Analysis*, VCH Publishers, New York.
24. Ellis, K. J., and Morrison, J. F. (1982) *Methods Enzymol. 87*, 405−426.
25. Lohse, D. L., Denu, J. M., Santoro, N., and Dixon, J. E. (1997) *Biochemistry 36*, 4568−4575.
26. Otwinowski, Z., and Minor, W. (1997) *Methods Enzymol. 276*, 307−326.
27. Collaborative Computational Project, No. 4 (1994) *Acta Crystallogr. D50*, 760−763.
28. Navaza, J. (1994) *Acta Crystallogr. A50*, 157−163.
29. Mohamadi, F., Richards, N. G. J., Guida, W. C., Liskamp, R., Lipton, M., Caufield, C., Chang, G., Hendrickson, T., and Still, W. C. (1990) *J. Comput. Chem. 11*, 4379−4386.
30. Chang, C., Guida, W. C., and Still, W. C. (1989) *J. Am. Chem. Soc. 111*, 4379−4386.
31. Still, W. C., Tempczyk, A., Hawley, R. C., and Hendrickson, T. (1990) *J. Am. Chem. Soc. 112*, 6127−6129.
32. Bruno, I. J., Cole, J. C., Lommerse, J. P., Rowland, R. S., Taylor, R., and Verdonk, M. L. (1997) *J. Comput.-Aided Mol. Des. 11*, 525−537.
33. Kole, H. K., Smyth, M. S., Russ, P. L., and Burke, T. R. (1995) *Biochem. J. 311*, 1025−1031.
34. Bilwes, A. M., Den Hertog, J., Hunter, T., and Noel, J. P. (1996) *Nature 382*, 555−559.
35. Hoffmann, K. M. V., Tonks, N. K., and Barford, D. (1997) *J. Biol. Chem. 272*, 27505−27508.
36. Yang, J., Liang, X., Niu, T., Meng, W., Zhao, Z., and Zhou, G. W. (1998) *J. Biol. Chem. 273*, 28199−28207.
37. Yang, J., Cheng, Z. L., Niu, T. Q., Liang, X. S., Zhao, Z. Z. J., and Zhou, G. W. (2000) *J. Biol. Chem. 275*, 4066−4071.
38. Bostrom, J., Norrby, P.-O., and Liljefors, T. (1998) *J. Comput.-Aided Mol. Des. 12*, 383−396.
39. Puius, Y. A., Zhao, Y., Sullivan, M., Lawrence, D. S., Almo, S. C., and Zhang, Z.-Y. (1997) *Proc. Natl. Acad. Sci. U.S.A. 94*, 13420−13425.
40. Taing, M., Keng, Y. F., Shen, K., Wu, L., Lawrence, D. S., and Zhang, Z. Y. (1999) *Biochemistry 38*, 3793−3803.
41. Seely, L., Staubs, P. A., Reichart, D. R., Berhanu, P., Milarski, K. L., Saltiel, A. R., Kusari, J., and Olefsky, J. M. (1996) *Diabetes 45*, 1379−1385.
42. Salmeen, A., Andersen, J. N., Myers, M. P., Tonks, N. K., and Barford, D. (2000) *Mol. Cell 6*, 1401−1412.

BI011389L